Strong-field ionization via a high-order Coulomb-corrected strong-field approximation

Michael Klaiber,[1,*] Jiří Daněk,[1] Enderalp Yakaboylu,[2] Karen Z. Hatsagortsyan,[1,†] and Christoph H. Keitel[1]
[1]*Max-Planck-Institut für Kernphysik, Saupfercheckweg 1, 69117 Heidelberg, Germany*
[2]*IST Austria (Institute of Science and Technology Austria), Am Campus 1, 3400 Klosterneuburg, Austria*
(Received 13 September 2016; published 2 February 2017)

Signatures of the Coulomb corrections in the photoelectron momentum distribution during laser-induced ionization of atoms or ions in tunneling and multiphoton regimes are investigated analytically in the case of a one-dimensional problem. A high-order Coulomb-corrected strong-field approximation is applied, where the exact continuum state in the S matrix is approximated by the eikonal Coulomb-Volkov state including the second-order corrections to the eikonal. Although without high-order corrections our theory coincides with the known analytical R-matrix (ARM) theory, we propose a simplified procedure for the matrix element derivation. Rather than matching the eikonal Coulomb-Volkov wave function with the bound state as in the ARM theory to remove the Coulomb singularity, we calculate the matrix element via the saddle-point integration method by time as well as by coordinate, and in this way avoiding the Coulomb singularity. The momentum shift in the photoelectron momentum distribution with respect to the ARM theory due to high-order corrections is analyzed for tunneling and multiphoton regimes. The relation of the quantum corrections to the tunneling delay time is discussed.

DOI: 10.1103/PhysRevA.95.023403

I. INTRODUCTION

In the strong-field ionization process of atoms and molecules, the Coulomb field of the atomic core plays a significant role for electron dynamics in the continuum and for the asymptotic photoelectron momentum distribution (PMD); see, e.g., [1,2]. Different schemes of attosecond spectroscopy [3,4] rely on PMD to derive information on the time-resolved atomic dynamics. Hence, an accurate description of Coulomb effects is of paramount importance for the strong-field theory. One of the main analytical tools in the strong-field theory is the so-called strong-field approximation (SFA) [5–7]. In the standard SFA, the effect of the Coulomb field of the atomic core for the continuum electron is neglected, describing it via the Volkov wave function [8], corresponding to the free electron in a plane laser field. Although including the effect of the Coulomb field of the atomic core by a perturbative approach in the standard SFA as a recollision was very insightful, providing an explanation for the nonsequential double ionization [9], high-order-harmonic generation [10], and recently the low-energy structures [11,12], the quantitative description of fine interference structures in PMD (see, e.g., [13]) requires a more accurate theory, accounting for Coulomb field effects nonperturbatively.

The Coulomb-corrected SFA (CCSFA) has been developed in [14,15], where the electron continuum state in the SFA amplitude is approximated by the eikonal Coulomb-Volkov state. The latter describes the electron in the laser and Coulomb fields, using the eikonal approximation [16] to treat the Coulomb field effect. The main difficulty of CCSFA mentioned above is that the phase of the continuum wave function has a singularity near the core and the wave function cannot be straightforwardly applied in the calculation of the SFA matrix element. The singularity is removed using the matching procedure of the eikonal Coulomb-Volkov wave function with the bound atomic state. More recently, a new version of CCSFA has been derived more systematically in [17–19], rigorously implementing the matching procedure in the analytical R-matrix (ARM) theory.

The aim of this paper is twofold. First, we extend CCSFA, considering high-order corrections to the eikonal wave function for the continuum electron, and employ it in CCSFA. We calculate PMD with the high-order CCSFA and discuss the impact of the corrections on PMD. Second, we propose a method to avoid the Coulomb singularity in CCSFA amplitude without using the complex matching procedure of the ARM theory. This is achieved by calculating the SFA matrix element via the saddle-point integration method not only by time, but also by coordinate. When neglecting the high-order corrections, our method provides results which coincide with the ARM theory.

The high-order Coulomb corrections to the eikonal Coulomb-Volkov wave function contain classical and quantum terms. Why is quantum correction to the eikonal Coulomb-Volkov wave function important? Recently a lot of experimental effort has been directed towards measuring the tunneling delay time during the laser-induced tunneling ionization [20–22]. The theoretical description of the tunneling delay time within a fully quantum theory is still missing. In the first-order eikonal CCSFA, the tunneling time is vanishing [23] because the tunneling is described within the Wentzel-Kramers-Brillouin (WKB) approximation where the wave function under the barrier is real. Then usually a combined quantum-classical consideration is applied to describe the tunneling delay time. The ionization is described quantum mechanically and the electron's further propagation in the continuum is described classically; see, e.g., [21]. In the quasistatic regime of tunneling ionization, the known Wigner formalism [24] can be applied to calculate the tunneling delay time as a energy derivative of the phase of the electron wave function under the barrier [25,26]. In the second step, the derived tunneling delay time is included into the initial conditions of the further classical

*klaiber@mpi-hd.mpg.de
†k.hatsagortsyan@mpi-hd.mpg.de

propagation. However, in the nonadiabatic regime, when the tunneling delay time is comparable with the laser period, the Wigner formalism is not applicable conceptually. In this case, there is a desire for a systematic description of the modification of PMD due to the ionization delay time. In this context, the quantum corrections in our CCSFA address the issue of the impact of the Coulomb field of the atomic core on quantum effects during ionization.

Note that the quantum recoil effects for the continuum electron at photon emission and absorption in a strong laser field have been first considered in [27] (the relativistic version in [28]). CCSFA based on this wave function was proposed in [29]; however, the final results were obtained only in the Born approximation.

The structure of the paper is the following. In Sec. II, the considered system is introduced. The scheme of CCSFA is discussed in Sec. III. The results in the zeroth- and first-order SFA are presented in Secs. IV and V. Comparisons with the ARM and Perelomov-Popov-Terent'ev (PPT) theories are given in Secs. VI and VII. Our main result—the second-order SFA containing quantum corrections—is presented in Sec. VIII. The relation of the high-order CCSFA to the ionization delay time is analyzed in Sec. IX, and to the heuristic quasiclassical theory of [30] in Sec. X.

II. THE CONSIDERED SYSTEM

We consider the ionization process of an atom (ion) in a strong laser field. Our description is one dimensional (1D). The active electron in the free atomic system is bounded by a 1D Coulomb potential,

$$V(x) = -\frac{Z}{|x|}, \tag{1}$$

with the nuclear charge Z. Atomic units are used throughout. Our aim is to develop a framework for high-order CCSFA for further extension in a 3D case. For this reason, rather than choose the very deeply bound ground state of a 1D atom [31,32], we assume that initially the 1D atom is in the first excited state with the Rydberg-like eigenenergy, $I_p = \kappa^2/2$, and with the following wave function [33]:

$$\langle x|\phi(t)\rangle = \frac{\kappa(2\kappa x)^{Z/\kappa}}{\sqrt{2Z\Gamma\left(\frac{2Z}{\kappa}\right)}}\exp(-\kappa|x| + iI_p t) \equiv c_a \exp[S_a(x,t)], \tag{2}$$

$$S_a(x,t) = -\kappa|x| + iI_p t + Z/\kappa \ln(2\kappa x), \tag{3}$$

$$c_a = \frac{\kappa}{\sqrt{2Z\Gamma\left(\frac{2Z}{\kappa}\right)}}. \tag{4}$$

Note that the electron ground-state wave function in a 1D soft-core potential has the same asymptotic form in the region $x \gg 1/\kappa$, relevant to our calculations.

In this paper, our intention is to describe the ionization step including the Coulomb effects at the tunnel exit. We do not consider Coulomb effects at recollisions. Therefore, the ionization of the atom is considered in a half-cycle laser pulse, where the recollisions are excluded explicitly:

$$F(t) = \begin{cases} E_0 \cos(\omega t) & \text{for } |\omega t| < \pi/2 \\ 0 & \text{for } |\omega t| \geqslant \pi/2, \end{cases} \tag{5}$$

with the laser field amplitude E_0 and frequency ω. However, our results are valid for a sinusoidal laser field when the contribution of the recollisions and the frustrated ionization are neglected. For the separation of the contribution of recollisions in the photoelectron dynamics, a restriction on the Keldysh parameter should be applied, $\gamma \lesssim 2$; see the derivation below in Sec. V. Note that our theory generalized in two or three dimensions would allow application for an elliptically polarized laser field without restriction on the Keldysh parameter because of lack of recollisions in that case.

We consider the nonrelativistic regime of the interaction when the typical electron momenta in the bound state as well as in the laser field are small with respect to the speed of light c: $\kappa/c \ll 1$ and $E_0/(c\omega) \ll 1$. We also exclude over-the-barrier ionization, which implies that the typical laser electric field E_s is much smaller with respect to the atomic field strength: $E_s/E_a < \kappa/16Z$, with $E_s = E_0$ in the tunneling ionization regime, $E_s = \gamma E_0$ in the multiphoton-ionization regime, $\gamma = \omega\kappa/E_0$ is the Keldysh parameter, and $E_a = \kappa^3$ is the atomic field. The depletion of the bound state is neglected. Finally, we assume that the photon energy is much less than the typical energies of the electron in the bound state I_p and in the laser field U_p: $\omega \ll I_p, U_p$ with the ponderomotive potential $U_p = E_0^2/(4\omega^2)$, which are necessary for application of the saddle-point integration (SPI) method in the calculation of the matrix element. Within these restrictions, we describe the ionization dynamics analytically with SFA, which will be explained in the following section.

III. HIGH-ORDER COULOMB-CORRECTED STRONG-FIELD APPROXIMATION

The dynamics of the electron is described by the Schrödinger equation in the length gauge,

$$i\partial_t|\psi(t)\rangle = H_0|\psi(t)\rangle - xF(t)|\psi(t)\rangle, \tag{6}$$

with the unperturbed atomic Hamiltonian,

$$H_0 = \frac{\hat{p}_x^2}{2} + V(x). \tag{7}$$

We calculate PMD $w(p) = |M(p)|^2$ analytically via the SFA amplitude [9],

$$M(p) = -i\int_{-\infty}^{\infty} dt\langle\psi_p(t)|xF(t)|\phi(t)\rangle, \tag{8}$$

where $|\psi_p(t)\rangle$ is the solution of Eq. (6) with the asymptotic momentum p. The approximate solution in the high-order eikonal approximation is found using the following ansatz:

$$\langle x|\psi_p(t)\rangle \equiv \psi_p(x,t) = \frac{\exp[iS(x,t)]}{\sqrt{2\pi}}. \tag{9}$$

The latter is inserted into the Schrödinger equation which yields an equation for the eikonal function S,

$$-\partial_t S = \frac{(\partial_x S)^2}{2} - xF + \alpha\left[V(x) - i\frac{\partial_{xx}S}{2}\right], \tag{10}$$

where we introduce an artificial perturbation parameter α, which we will set to unity later, such that we consider the Coulomb potential as well as the quantum correction perturbatively. Foreseeing the subsequent calculation, we can insert the typical value for the coordinate $x \sim \sqrt{\kappa/E_s}$ and time $t \sim \kappa/E_s$ into the perturbation of the original differential equation, $V \sim Z/x \sim Z\sqrt{E_s/\kappa}$ and $\partial_{xx}S \sim Vt/x^2 \sim Z\sqrt{E_s/\kappa}$, and see that the quantum term is of the same order as the potential one and the simultaneous perturbative treatment of both of the terms is justified when $E_0 \ll E_a$; see Eq. (22) in [34].

In the usual eikonal approximation, in particular in [14,17], the last quantum term $\partial_{xx}S$ is neglected and the atomic potential is treated perturbatively in the eikonal equation (10). In contrast to that, we include and take into account the quantum term, as well as the atomic potential by perturbation theory. The quantum term yields a correction to the eikonal $S(x,t)$ of the second order. Therefore, we also have to include in the solution of the eikonal the second-order correction due to the atomic potential. With the ansatz

$$S = S_0 + \alpha S_1 + \alpha^2 S_2, \tag{11}$$

the zeroth-, first-, and second-order equations read

$$-\partial_t S_0 = \frac{(\partial_x S_0)^2}{2} - xF, \tag{12}$$

$$-\partial_t S_1 = \partial_x S_0 \partial_x S_1 + V - i\frac{\partial_{xx} S_0}{2}, \tag{13}$$

$$-\partial_t S_2 = \frac{(\partial_x S_1)^2}{2} + \partial_x S_0 \partial_x S_2 - i\frac{\partial_{xx} S_1}{2}. \tag{14}$$

The zeroth-order equation is the Hamilton-Jacobi equation for the electron in the laser fields, which provides the well-known Volkov action [8] for the electron in the laser field,

$$S_0(x,t) = [p + A(t)]x + \int_t^{t_f} dt' \frac{[p + A(t')]^2}{2}. \tag{15}$$

The first- and second-order equations are solved with the method of characteristics:

$$\begin{aligned} S_1(x,t) &= \int_t^{t_f} dt' V(x(t')), \\ S_2(x,t) &= \int_t^{t_f} dt' \frac{\left[\int_{t'}^{t_f} dt'' \partial_x V(x(t''))\right]^2}{2} \\ &\quad - i\int_t^{t_f} dt' \int_{t'}^{t_f} dt'' \frac{\partial_{xx} V(x(t''))}{2}, \end{aligned} \tag{16}$$

where $x(t') = x + \int_t^{t'} ds[p + A(s)]$ is the electron classical trajectory in the laser field solely, and $A(t)$ is the laser vector potential, with $F(t) = \partial_t A(t)$. Whereas S_1 is a correction to the phase of the ionizing electron due to the Coulomb potential energy along the laser-driven trajectory, the (first) classical term in S_2 accounts for the perturbation of the Coulomb energy due to the perturbation of the trajectory by the Coulomb field.

Further, we note that the terms in S_0, S_1 and the first term in S_2 are quasiclassical terms of the order of $1/\hbar$, and the second summand in S_2 is a quantum term of the order of $\hbar^0$. The latter is a special feature of the 1D system. In a 3D Coulomb system, this term does not exist due to the fact that $\Delta V(r) = 0$ for $r > 0$.

We insert our approximate wave function for the continuum electron into the SFA amplitude of Eq. (8). The two-dimensional integration in the matrix element is carried out by the SPI method (the applicability of SPI for S_0 CCSFA is discussed in Sec. IV). For the latter, we exponentiate the whole expression,

$$\begin{aligned} M(p) = -\frac{ic_a}{\sqrt{2\pi}} \int dt dx \exp\{-iS^*(x,t) \\ + \ln[xF(t)] + S_a(x,t)\}, \end{aligned} \tag{17}$$

where * indicates complex conjugation. The saddle-point conditions

$$\begin{aligned} \left.\frac{d\zeta(x,t)}{dt}\right|_{(t,x)=(t_s,x_s)} &= 0, \\ \left.\frac{d\zeta(x,t)}{dx}\right|_{(t,x)=(t_s,x_s)} &= 0, \end{aligned} \tag{18}$$

with $\zeta(x,t) = -iS^*(x,t) + \ln[xF(t)] + S_a(x,t)$, define the saddle points (t_s,x_s) around which the exponent is quadratically expanded in SPI. To be consistent with the expansion of $S(x,t)$, we also expand the saddle points (t_s,x_s) up to second order,

$$\begin{aligned} t_s &= t_s^{(0)} + \alpha t_s^{(1)} + \alpha^2 t_s^{(2)}, \\ x_s &= x_s^{(0)} + \alpha x_s^{(1)} + \alpha^2 x_s^{(2)}, \end{aligned} \tag{19}$$

and solve the saddle-point equations perturbatively. The corresponding zeroth-, first-, and second-order functions in the exponent are

$$\begin{aligned} \zeta_0(x,t) &= -iS_0(x,t) + \ln[xF(t)] + S_{a,0}(x,t), \\ \zeta_1(x,t) &= -iS_1(x,t) + S_{a,1}(x), \\ \zeta_2(x,t) &= -iS_2^*(x,t), \end{aligned} \tag{20}$$

with $S_{a,0}(x,t) = -\kappa x + iI_p t$, $S_{a,1}(x) = Z/\kappa \ln[2\kappa x]$. Therefore, the zeroth-order saddle-point equations read

$$-\partial_t S_0(x,t) = -I_p + i\frac{F'(t)}{F(t)}, \tag{21}$$

$$\partial_x S_0(x,t) = i\left(\kappa - \frac{1}{x}\right). \tag{22}$$

The zeroth-order $(t_s^{(0)},x_s^{(0)})$ solution is found numerically. The higher-order equations are solved analytically and the solutions as well as the SFA amplitude $M(p)$ are expressed by $(t_s^{(0)},x_s^{(0)})$.

We may estimate the zeroth-order solution in a cosine-electric field as $t_s^{(0)} \sim \arcsin[i\kappa\omega/E_0]/\omega - i/\sqrt{\kappa E_s}$ and $x_s^{(0)} \sim \sqrt{\kappa/E_s}$, which correspond to the solutions in the case of a short-range potential. One can give a physical interpretation for x_s as the point where the ionization starts, i.e., at $x < x_s$ the bound state is undisturbed, and at $x > x_s$ there is a nonzero outgoing current. At any value of the Keldysh parameter, the starting point of the ionization x_s is smaller than the exit coordinate, $x_s \ll x_e$. In fact, the exit coordinate for any

γ is $x_e = (2/\gamma^2)(\sqrt{1+\gamma^2}-1)(I_p/E_0)$ [35]. Consequently, $x_s/x_e \sim \sqrt{E_0/E_a} \ll 1$ at $\gamma \ll 1$, and $x_s/x_e \sim \sqrt{\omega/I_p} \ll 1$ at a large γ. Note that the saddle point x_s is also far away from the atomic core, $x_s\kappa \gg 1$, and therefore, the eikonal $S_1(x_s,t)$ is not singular. Thus, the electron always starts ionization under the barrier far away from the core, but also far away from the exit, $1/\kappa \ll x_s \ll x_e$. It is an analog to the matching coordinate in ARM that fulfills the same conditions.

The derivation of the higher-order corrections to the saddle points is straightforward, but cumbersome, and yields a large analytical expression. We give only the structure of the first-order solution of the (t,x) saddle points,

$$t_s^{(1)} = \left.\frac{-\partial_{xt}\zeta_0\partial_x\zeta_1 + \partial_t\zeta_1\partial_{xx}\zeta_0}{\partial_{xt}\zeta_0^2 - \partial_{tt}\zeta_0\partial_{xx}\zeta_0}\right|_{x=x_s^{(0)},t=t_s^{(0)}},$$

$$x_s^{(1)} = \left.\frac{\partial_{tt}\zeta_0\partial_x\zeta_1 - \partial_t\zeta_1\partial_{xt}\zeta_0}{\partial_{xt}\zeta_0^2 - \partial_{tt}\zeta_0\partial_{xx}\zeta_0}\right|_{x=x_s^{(0)},t=t_s^{(0)}}. \tag{23}$$

The structure of the SFA amplitude up to second order is the following:

$$M(p) \approx -ic_a\frac{\sqrt{2\pi}}{\sqrt{\det\zeta}}\exp\left[\left(\zeta_0+\alpha\zeta_1+\alpha^2\zeta_2+\alpha^2\frac{\partial_{xx}\zeta_0\partial_t\zeta_1^2 - 2\partial_x\zeta_1\partial_{xt}\zeta_0\partial_t\zeta_1 + \partial_{tt}\zeta_0\partial_x\zeta_1^2}{2\left(\partial_{xt}\zeta_0^2 - \partial_{tt}\zeta_0\partial_{xx}\zeta_0\right)}\right)\Bigg|_{(x_s^{(0)},t_s^{(0)})}\right], \tag{24}$$

where $\det\zeta$ is the Van Vleck–Pauli–Morette [36] determinant of the matrix formed by the second-order derivatives of ζ,

$$\det\zeta = \det\begin{pmatrix}\partial_{xx}\zeta & \partial_{xt}\zeta\\ \partial_{tx}\zeta & \partial_{tt}\zeta\end{pmatrix}. \tag{25}$$

$2\pi/\sqrt{\det\zeta}$ arises from SPI and represents intuitively the typical size of the volume element $dxdt$.

Finally, we determine the maximum of PMD via the extremum condition,

$$\left.\frac{\partial w(p)}{\partial p}\right|_{p=p_m} = 0, \tag{26}$$

which is solved again perturbatively, $p_m = p_m^{(0)} + \alpha p_m^{(1)} + \alpha^2 p_m^{(2)}$, providing the maximum of the probability amplitude,

$$M(p_m) \sim \left.\frac{\exp(\zeta)}{\sqrt{\det\zeta}}\right|_{p=p_m}, \tag{27}$$

with the function in the exponent being expanded up to second order. In the next section, we will discuss the results of the calculations. The results obtained in the nth $-$ order expansion are referred to as S_n CCSFA.

IV. S_0 CCSFA

The ionization amplitude in the zeroth order,

$$M(p) \sim \frac{\exp(\zeta_0)}{\sqrt{\det\zeta_0}}, \tag{28}$$

corresponds to the standard SFA describing the ionization from short-range potentials with $Z \ll \kappa$. As a check of accuracy for our SPI, we calculate analytically the S_0 CCSFA amplitude for a cosine-laser pulse and compare it with the PPT result [37]. The saddle point for the most probable final momentum, i.e., the position and time where and when the ionization dynamics starts, can be given approximately analytically, where higher-order terms in E_0/E_a are dropped,

$$x_s^{(0)} \approx \sqrt{\frac{\kappa}{E_s}}, \tag{29}$$

$$t_s^{(0)} \approx \frac{\arcsin[i\gamma]}{\omega} - \frac{i}{\sqrt{\kappa E_s}}. \tag{30}$$

The latter provides PMD for ionization from a short-range potential in the leading terms in E_0/E_a,

$$w(p) = \frac{\pi\kappa^2}{eE_s}\exp\left[-\frac{\kappa^3(-\sqrt{\gamma^2+1}\gamma+2\gamma^2\sinh^{-1}\gamma+\sinh^{-1}\gamma)}{2\gamma^3E_0} - \frac{(p-p^{(0)})^2}{\Delta^2}\right], \tag{31}$$

where

$$p^{(0)} = \int_0^\infty dt\,F(t) = \frac{E_0}{\omega} \tag{32}$$

is the most probable momentum, $E_s = E_0\sqrt{1+\gamma^2}$, and

$$\Delta = \frac{\sqrt{E_s}}{\sqrt{\kappa[\sqrt{1+1/\gamma^2}\sinh^{-1}(\gamma)-1]}} \tag{33}$$

is the width of the momentum distribution. We note that the derived ionization amplitude differs from the PPT result in a short-range potential by a constant factor of $\pi/e \approx 1.16$, which arises due to the approximate x integration with SPI in contrast to the exact x integration in PPT. The SPI error mainly arises due to the Gaussian x-integration region $(-\infty,\infty)$ and can be reduced to a factor of $[1+\mathrm{erf}(1)]^2\pi/4e \approx 0.98$ (cf. with Eq. (8.16) of Chap. 3 in Ref. [38]), when the integration spans only over the relevant region of the coordinate $(0,\infty)$. In fact, the region behind the atomic core ($x<0$) does not contribute to the ionization. In the high-order calculations, the integration region will be restricted in the same way. The application of SPI does not change the scaling of the probability with respect to the laser and atom parameters, but only gives an approximate overall factor. The latter is also the case in high-order CCSFA.

Generally, the saddle-point approximation by time can be improved by including the third-order term $\partial_{ttt}\zeta_0(x_s^{(0)},t_s^{(0)})(t-t_s^{(0)})^3/6$ in the integration around the saddle point. However, the analysis of this term shows that it has no influence on the momentum distribution of the ionized electron, and changes the ionization probability only insignificantly due its relative smallness that can be estimated by $(E_0/E_a)/72$.

V. S_1 CCSFA

The Coulomb field effect on PMD is described by the first-order correction terms to the eikonal wave function. The correction that leads to a qualitative change compared to the short-range potential case is the first-order Coulomb-correction ζ_1 in the exponent,

$$\frac{\exp(\zeta_0+\zeta_1)}{\sqrt{\det\zeta_0}}. \tag{34}$$

Note that the preexponential term $\det\zeta_1$ yields a contribution which is small compared to the leading term in the order of E_0/E_a and is neglected in S_1 CCSFA. This term is included in the wave function of the next order, and its effect will be discussed in S_2 CCSFA.

The Coulomb-correction term in S_1 CCSFA, $\exp(\zeta_1)$, has two consequences. First, $\exp(\zeta_1)$ changes the magnitude of the ionization probability via the following correction factor:

$$\begin{aligned}\left|\frac{c_a}{c_{a,0}}\exp\left[\zeta_1\left(x_s^{(0)},t_s^{(0)}\right)\right]\right|^2 &\approx \frac{4^{Z/\kappa}\left(\frac{1}{\sqrt[4]{\gamma^2+1}\sqrt{f}}\right)^{\frac{2Z}{\kappa}}}{\Gamma\left(\frac{2Z}{\kappa}+1\right)}\\ &\times\exp\left\{\frac{4Z}{\kappa}\coth^{-1}\left[\frac{(\sqrt{\gamma^2+1}-1)}{\gamma}\right.\right.\\ &\left.\left.\times\coth\left(\frac{\sinh^{-1}(\gamma)}{2}-\frac{\gamma\sqrt{f}}{2\sqrt[4]{\gamma^2+1}}\right)\right]\right\}.\end{aligned} \tag{35}$$

The expression above contains high-order E_0/E_a terms which should be neglected within the S_1 SFA. When the leading E_0/E_a term is maintained, one arrives at the final result of S_1 SFA,

$$\left|\frac{c_a}{c_{a,0}}\exp\left[\zeta_1\left(x_s^{(0)},t_s^{(0)}\right)\right]\right|^2 \approx \frac{16^{Z/\kappa}\left(\frac{E_0}{\kappa^3}\right)^{-\frac{2Z}{\kappa}}}{\Gamma\left(\frac{2Z}{\kappa}+1\right)}, \tag{36}$$

with $c_{a,0}=\sqrt{\kappa/2\pi}$. We note that the ionization amplitude of S_0 CCSFA given by Eq. (31), with the correction factor of S_1 CCSFA given by Eq. (36), reproduces the PPT-ionization rate [37,39].

Second, ζ_1 yields a shift of the momentum distribution due to a momentum transfer to the Coulomb potential during the motion of the ionized electron in the continuum immediately after leaving the tunnel exit (we emphasize again that here recollisions are not considered). The momentum shift derived from the condition of the extremum of $M(p)$, given by Eq. (26), with S_1 CCSFA, is shown in Fig. 1. We can also give an analytical estimation of the momentum shift via $\partial_x\zeta_1$. It consists of two terms. The first arises during the motion in the half-cycle laser pulse and will be called $\Delta p_C^{(1)}$, and the second $\Delta p_C^{(2)}$ during the motion in the field-free time region

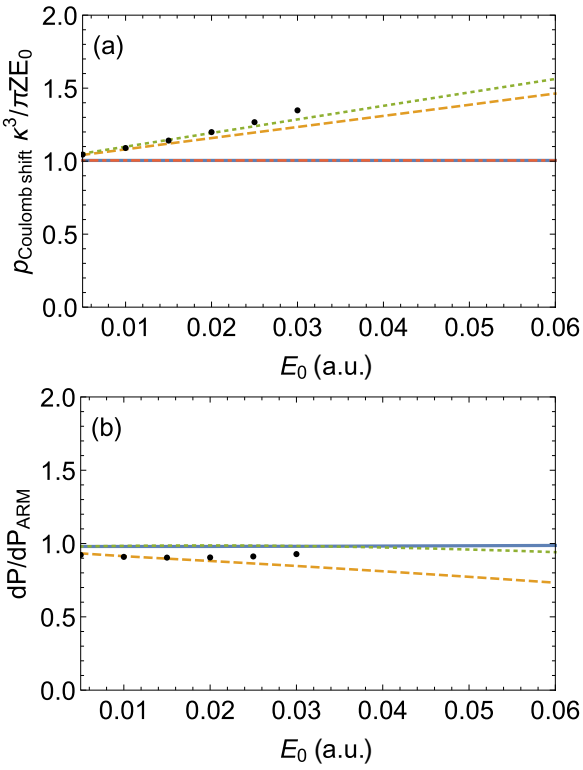

FIG. 1. (a) The Coulomb momentum shift vs the laser field strength in the quasistatic regime $\gamma=0.1$, $Z/\kappa=1$ with the quasiclassical S_1 CCSFA (solid line), the quasiclassical S_2 CCSFA (dashed line), the quantum S_2 CCSFA (dotted line), and the ARM theory which coincides exactly with the curve via the S_1 CCSFA (dot-dashed line). The black dots display the result of the method of Sec. X. (b) The ratio of the ionization rate at the peak of the momentum distribution to the corresponding ARM-ionization rate in the quasistatic regime $\gamma=0.1$, $Z/\kappa=1$ for the quasiclassical S_1 CCSFA (solid line), the quasiclassical S_2 CCSFA (dashed line), and the quantum S_2 CCSFA (dotted line). The black dots display the result of the method of Sec. X.

after the laser pulse,

$$\begin{aligned}\Delta p_C^{(1)} &= \frac{E_0 Z}{2\sqrt{\gamma^2+1}\kappa^3}\left[\pi\gamma^2-2(\gamma^2+1)\tan^{-1}(\gamma)\right.\\ &+2(\gamma^2+1)\tan^{-1}\frac{\gamma-i}{\sqrt{\gamma^2+1}}+2(\gamma^2+1)\\ &\left.\times\tan^{-1}\frac{\gamma+i}{\sqrt{\gamma^2+1}}+2\gamma+\pi\right],\\ \Delta p_C^{(2)} &= \frac{E_0 Z\gamma^3}{\sqrt{1+\gamma^2}\kappa^3},\end{aligned} \tag{37}$$

which in the static regime, $\gamma\ll 1$, is

$$\begin{aligned}\Delta p_C^{(1)} &\approx \frac{\pi Z E_0}{\kappa^3},\\ \Delta p_C^{(2)} &= 0,\end{aligned} \tag{38}$$

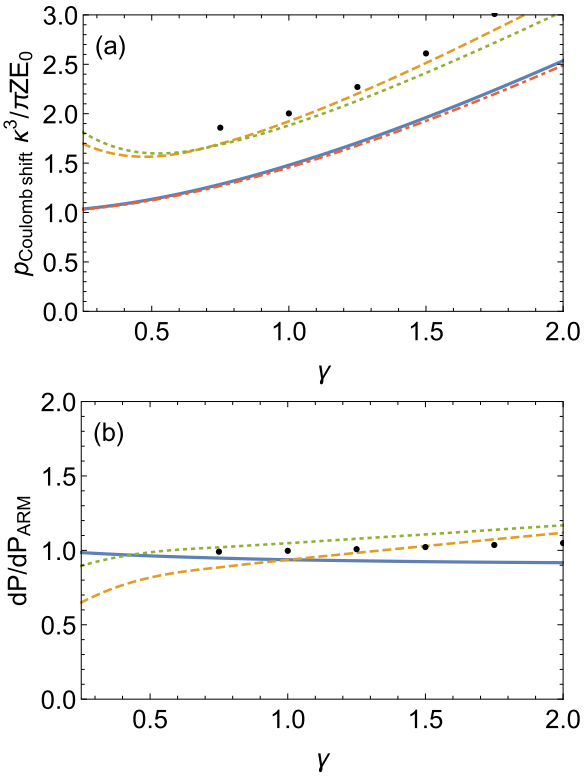

FIG. 2. (a) The Coulomb momentum shift vs the Keldysh parameter γ in the nonadiabatic regime $\omega = 0.02$, $Z/\kappa = 1$ with the quasiclassical S_1 CCSFA (solid line), the quasiclassical S_2 CCSFA (dashed line), the quantum S_2 CCSFA (dotted line), and for the ARM theory (dot-dashed line). (b) The ratio of the ionization rate at the peak of the momentum distribution to the corresponding ARM-ionization rate vs the Keldysh parameter γ in the nonadiabatic regime $\omega = 0.02$, $Z/\kappa = 1$ for the quasiclassical S_1 CCSFA (solid line), the quasiclassical S_2 CCSFA (dashed line), and the quantum S_2 CCSFA (dotted line). The black dots display the result of the method of Sec. X.

and in the nonadiabatic regime, $\gamma \gtrsim 1$, is

$$\Delta p_C^{(1)} \approx \frac{\pi Z E_0}{\kappa^3}\left(\frac{\gamma}{2} + \frac{1}{4\gamma} + \frac{2}{\pi}\right),$$
$$\Delta p_C^{(2)} \approx \frac{\gamma^2 Z E_0}{\kappa^3}. \tag{39}$$

In the latter, the electron trajectory $x(t) \approx x_e + E_0 t/\omega$ can be used taking into account that the drift during the half-cycle pulse from $t = 0$ up to $T = \pi/2\omega$ is small compared to the tunnel exit x_e and can be dropped. When $\Delta p_C^{(2)} \ll \Delta p_C^{(1)}$, which according to Eq. (39) is fulfilled at $\gamma \lesssim 2$, the initial Coulomb momentum transfer can be separated from further Coulomb effects. At the same condition, the initial Coulomb momentum transfer can be separated from the Coulomb momentum transfer at the laser-driven recollision in the case of a sinusoidal laser field. Thus, our results related to the initial Coulomb momentum transfer are valid up to $\gamma \lesssim 2$ for a sinusoidal laser field. We emphasize again that we do not consider the Coulomb effects at the laser-driven recollisions and the frustrated ionization in this manuscript.

Figures 1(a) and 2(a) show the Coulomb momentum shift estimated by Eqs. (38) and (39). The Coulomb momentum shift relative to the characteristic photoelectron momentum in a laser field, E_0/ω, is derived by multiplying the values in Figs. 1(a) and 2(a) by the factor $\pi Z\omega/\kappa^3$. One can observe that the Coulomb momentum shift almost exactly corresponds to the S_1 CCSFA theory. Physically, this result can be interpreted as a verification of the simple-man model [40], where instantaneous tunneling up to the exit x_e is followed by classical propagation in the continuum, where the Coulomb field of the atomic core induces a momentum shift,

$$\Delta p_C \approx -\int_0^\infty dt\, \partial_x V(x(t)). \tag{40}$$

The latter expression yields Eqs. (38) and (39) when the electron trajectory $x(t)$ is used with either static or nonadiabatic tunnel exit coordinate. In the nonadiabatic regime, the Coulomb momentum shift is larger than in the quasistatic case (see Fig. 2) because the nonadiabatic trajectory is close to the atomic core for a longer time interval.

The approach of S_1 CCSFA is physically equivalent to the ARM theory. The only difference is in how the Coulomb singularity is treated. While in the ARM theory a rigorous matching of the electron wave function in the continuum to the bound state is employed, in the S_1 CCSFA, the Coulomb singularity is avoided by simply using additional SPI for the coordinate integration. In the next section, we provide in detail the comparison of S_1 CCSFA with ARM.

VI. COMPARISON OF S_1 CCSFA WITH ARM THEORY

We provide a comparison of the ARM theory [17] with S_1 CCSFA in Figs. 1 and 2, where the most probable momentum and the corresponding rate are shown. The figures indicate that the results of S_1 CCSFA and ARM for the most probable momentum as well as for the rate are mostly identical. There is only a slight difference in the most probable momentum and in the ionization rate in the nonadiabatic regime at large γ. To understand why this slight difference arises, let us look at the details. In the derivation of the ionization amplitude in the ARM theory, one arrives at the following expression for the amplitude:

$$M^{ARM}(p) = -i\int dt \frac{\kappa c_a}{\sqrt{2\pi}} \times \exp[-iS_0(b,t) - iS_1(b,t) + S_a(b,t)] \tag{41}$$

(this equation is the 1D analog of Eq. (28) of [17]), where b is the matching point of the bound and the continuum states, and the amplitude is approximately independent of the parameter b. The latter implies that the exponent in the expression fulfills the SPI condition at b. Using SPI for the time integration yields

$$M^{ARM}(p) \approx -i\kappa c_a \sqrt{\frac{1}{-\partial_{tt} S_0(b,t_s)}} \times \exp[-iS_0(b,t_s) - iS_1(b,t_s) + S_a(b,t_s)], \tag{42}$$

with $-\partial_{tt} S_0(b,t_s) \approx \kappa E_s$.

On the other side, the SPI over the time and coordinate in our S_1 CCSFA yields

$$M(p) \approx i c_a x_s^{(0)} F\left(t_s^{(0)}\right) \frac{\sqrt{2\pi}}{\sqrt{-\det \zeta\,|_{\left(x_s^{(0)},t_s^{(0)}\right)}}} \times \exp\left[-i S_0\left(x_s^{(0)},t_s^{(0)}\right) - i S_1\left(x_s^{(0)},t_s^{(0)}\right) + S_a\left(x_s^{(0)},t_s^{(0)}\right)\right], \tag{43}$$

where $-\det \zeta\,|_{x_s^{(0)},t_s^{(0)}} \approx 2E_s^2$.

For comparison of Eqs. (42) and (43), we use $b = x_s^{(0)}$ as the ARM amplitude does not depend on the matching point within the barrier near the condition of the coordinate SPI.

In the further derivation of the final ARM expression in [17], the factor $\exp(-E_s b^2/2\kappa)$ is neglected and, after this operation, the SFA amplitude, estimated for the typical values for $x_s^{(0)} \sim \sqrt{\kappa/E_s}$ and $F(t_s^{(0)}) \sim E_s$, differs from the ARM amplitude by a constant factor $\sqrt{\pi/e}$, which is close to unity.

Thus, the reason for a small difference between the ARM and S_1 CCSFA theories is that in the S_1 CCSFA, SPI with respect to the coordinate is applied, which implies that higher-order derivatives with respect to x are neglected. Meanwhile, in the ARM theory, a term $\exp(-E_s b^2/2\kappa)$ is neglected which is of the same order. Therefore, the ARM and S_1 CCSFA theories are of the same accuracy.

VII. THE PPT COULOMB-CORRECTION FACTOR IN THE NONADIABATIC REGIME

We stated in Sec. V that S_1 CCSFA provides a Coulomb-correction factor for the ionization amplitude which coincides with the PPT theory [37]. Recently, a modification for the Coulomb-correction factor to the PPT theory was calculated in the nonadiabatic regime [41]. This factor is absent in our S_1 SFA because it accounts for the effect of frustrated ionization [42,43], i.e., the capture of low-energy electrons in the Coulomb potential of the atomic core after switching off the laser field; meanwhile, we neglect all Coulomb effects far from the tunnel exit (rescatterings and frustrated ionization).

To confirm that the additional Coulomb-correction factor of [41] is due to frustrated ionization, one may derive this factor heuristically, in analogy to the derivation in [35]. In the asymptotic PMD after switching off the laser field, only electrons which gain sufficient energy in the laser field can leave the Coulomb potential. This energy gain depends on the ionization time, $\varepsilon_e \sim A(t_i)^2/2$, with the ionization time t_i, and the laser vector potential of the sinusoidal field $A(t) = E_0/\omega \sin(\omega t)$, and has to be larger than the negative Coulomb energy: $\varepsilon_e > Z/x_e = Z/\kappa\omega$. In the latter, we take into account that the minimum of the asymptotic coordinate cannot be smaller than the tunnel exit coordinate. From this it follows that electrons that tunnel close to the peak of the laser field are captured by the Coulomb potential and will not be detected. Only electrons with a certain ionization time away from the peak will be ionized. The reduction factor of the ionization rate due to the capturing can therefore be estimated via Eq. (31) at $\gamma \gg 1$,

$$\left|\frac{M(-A(t_i))}{M(0)}\right|^2 \approx \left(\frac{2\gamma}{e}\right)^{-2Z/\kappa}, \tag{44}$$

which coincides with the additional factor derived in [41]. As our calculations do not include recollisions and the effect of the frustrated ionization, this factor does not appear in our calculations.

VIII. S_2 CCSFA

The S_1 CCSFA considered up to now provides results of PPT and ARM theories, circumventing the necessity of the wave-function matching procedure. The coincidence of the results is due to the fact that the saddle point of the coordinate SPI is rather far from the atomic core, where the eikonal wave function for the electron is still valid. In this section, we account for high-order corrections in the CCSFA approach to go beyond the known results of PPT and ARM theories.

The S_2 CCSFA contains a quasiclassical correction term ($\sim 1/\hbar$) as well as quantum correction terms ($\sim \hbar^0$). One quantum correction term is in the S_2 term of the eikonal, and the second is in the ionization amplitude due to the S_1 term in the prefactor (determinant), which has been neglected in S_1 CCSFA because of smallness; see Eq. (34). The SFA that includes only the quasiclassical correction term in the second order will be called quasiclassical S_2 CCSFA, whereas the CCSFA with all correction terms will be called the quantum S_2 CCSFA.

The second-order corrections to the ionization amplitude are small and change the momentum distribution only quantitatively. The shift of the peak of PMD and the change of probability at the peak of the momentum distribution due to these terms are displayed for the quasistatic regime in Fig. 1, and for the nonadiabatic regime in Fig. 2. In both regimes, the second-order correction terms do not change the ionization probability significantly, but increase the Coulomb momentum shift compared to the S_1 CCSFA result.

The three different correction terms have a distinct physical origin. The second-order terms in the quasiclassical S_2 CCSFA decrease the ionization probability and increase the momentum shift. These changes are due to the decreases of the effective potential barrier formed by the Coulomb field of the atomic core and the laser field. In fact, the tunnel exit coordinate taking into account the Coulomb field can be found from the relation

$$-I_p = -E_0 x - \frac{Z}{|x|}, \tag{45}$$

which can be solved exactly in x. An expansion of this solution in E_0/E_a gives

$$x_e \approx \frac{I_p}{E_0}\left(1 - \frac{4ZE_0}{\kappa E_a}\right). \tag{46}$$

The S_1 CCSFA contains the simple-man exit $x_e \approx I_p/E_0$, while in S_2 CCSFA the tunnel exit shifts closer to the atomic core due to the Coulomb correction according to the term of the order of E_0/E_a. This effect increases the Coulomb momentum shift in the continuum according to Eq. (40).

Due to the Coulomb field effect according to the second-order quasiclassical corrections, the tunneling probability decreases because of larger damping from the tunneling exponent $\exp(-\int |p(x)|dx)$, with $p(x) = i\sqrt{2(I_p - xE_0 + Z/|x|)}$. The same can be deduced from the SFA formalism. The

decrease of the ionization probability is mainly due to the next-to-leading-order E_0/E_a corrections in the Coulomb-correction factor neglected in the S_1 CCSFA (the second term in the bracket),

$$\left|\frac{c_a}{c_{a,0}}\exp\left[\zeta_1\left(x_s^{(0)},t_s^{(0)}\right)\right]\right|^2 \approx \frac{1}{2}\left(\frac{4\kappa^3}{E_0}-2\kappa x_s^{(0)}\right)^{\frac{2Z}{\kappa}}. \quad (47)$$

From this formula, one can observe that the Coulomb-correction factor decreases with an increasing saddle point $x_s^{(0)}$, which fits the intuitive explanation above.

The quantum correction to S_2 increases the tunneling probability, which can be understood intuitively as a decrease of the tunneling barrier. In fact, the quantum correction term $-i\partial_{xx}S/2 \sim -ip'(x)$ in Eq. (10) is equivalent to an additional term in the effective potential $V_{\rm eff} = V - xF(t) - i\partial_{xx}S/2$, which decreases the effective potential and consequently the coordinate of the tunnel exit. From this, it follows that quantum corrections increase the ionization probability and the Coulomb momentum shift in the continuum motion.

IX. RELATION TO THE IONIZATION DELAY TIME

Let us inspect the role of the different Coulomb quantum correction terms in the ionization amplitude: the quantum term in S_2 and the correction term in the determinant due to high-order terms originating from S_1. We observe that for the Coulomb momentum shift in both regimes, the quasiclassical S_2 and quantum S_2 curves are very close to each other; see Figs. 1(a) and 2(a). This indicates that the two quantum corrections almost compensate each other. Whereas the quantum term in S_2 increases the momentum shift, the correction term in the determinant decreases it, yielding to an approximately net zero change. The role of the quantum correction due to the determinant term is further clarified in Fig. 3. The compensation is different in the quasistatic and nonadiabatic regimes. While in the quasistatic regime the overall momentum shift is positive (the determinant term contribution is less important), in the nonadiabatic regime the net momentum corrections are negative (the determinant term contribution is more conspicuous).

Physically the momentum shifts can be interpreted as a delay time at the detector in the attoclock-type setup [20] with respect to the simple-man model prediction. The quantum correction term in S_2 induces a positive delay time and the determinant term induces a negative delay time of the same order in comparison to the simple-man result given by the quasiclassical S_2 CCSFA. We emphasize that the delay time due to the Coulomb quantum corrections is an additional effect on top of the Wigner delay time [24] at tunneling ionization [26]. The latter is not described by CCSFA.

In the more realistic 3D case, the quantum correction in S_2 is vanishing as the term $\Delta V(r) = 0$ in Eq. (13) for the 3D Coulomb potential. Then, in the 3D case, the overall delay time due to Coulomb quantum corrections will be connected only with the determinant term and, consequently, will be negative. Moreover, one can show that the time derivatives of $S(x,t)$ in the determinant are responsible for the negative delay time, whereas spatial derivatives play a minor role for this effect. This indicates that the negative delay time due to Coulomb quantum corrections is not connected with the spatial uncertainty of the bound state, but is an effect due to quantum corrections in the continuum state. Furthermore, one observes from Fig. 3 that the delay time effect increases in the near-threshold regime (large E_0/E_a), whereas in the deep-tunneling regime, it is not significant. These are in line with the specific properties of the tunneling ionization delay time [26].

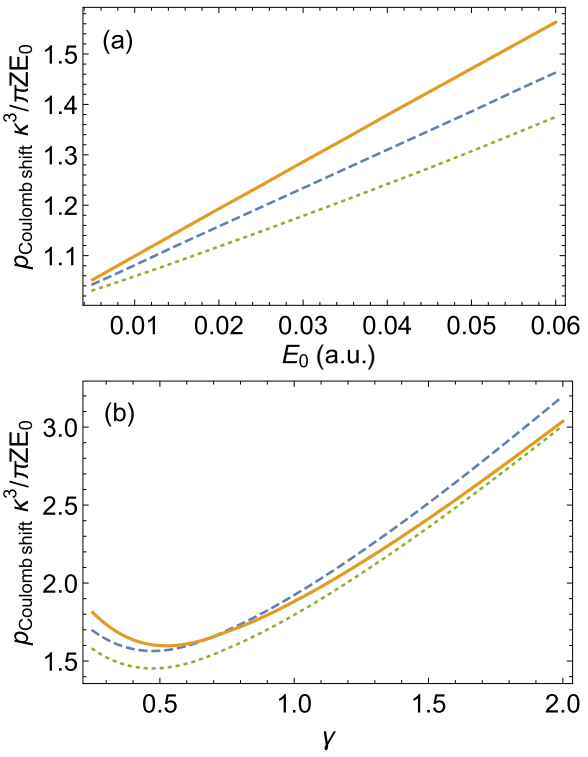

FIG. 3. (a) The Coulomb momentum shift of the final momentum vs the laser field in the quasistatic regime of $\gamma = 0.1$ via classical S_2 CCSFA (dashed line), quantum S_2 CCSFA including both quantum corrections (solid line), and quantum SFA where the quantum corrections in the exponent are dropped (dotted line). (b) The Coulomb momentum shift of the final momentum vs γ in the nonadiabatic regime of $\omega = 0.02$ a.u. via classical S_2 CCSFA (dashed line), quantum S_2 CCSFA including both quantum corrections (solid line), and quantum SFA where quantum corrections in the exponent are dropped (dotted line).

X. COMPARISON WITH THE HEURISTIC QUASICLASSICAL METHOD

Finally, we discuss the relation of the results of our systematic S_n CCSFA with the heuristic quasiclassical approach (HQA) of Ref. [30] for a nonperturbative treatment of Coulomb field effects during the under-the-barrier motion in strong-field ionization.

Briefly recalling HQA, we begin with the ionization probability expressed via the quasiclassical propagator,

$$M(p) = i\int dx_f dx dt\,\exp(-ipx_f)G(x_f,x,t_f,t) \times xF(t)\frac{\phi_0(x,t)}{\sqrt{2\pi}}, \quad (48)$$

with the quasiclassical Green's function,

$$G(x_f,x,t_f,t)=\sqrt{\frac{i\partial_{x_f,x}\tilde{S}_c}{2\pi}}\exp(i\tilde{S}_c), \tag{49}$$

and the quasiclassical action, evaluated along the classical trajectory corresponding to the most probable electron,

$$\tilde{S}_c=\int_t^{t_f}dt\left[\frac{\dot{x}(t)^2}{2}+xF(t)-V(x)\right]. \tag{50}$$

The x_f integral in Eq. (48) can be calculated via SPI, yielding

$$M(p)=\frac{i}{\sqrt{2\pi}}\int dxdt\exp(-ipx_f+i\tilde{S}_c)xF(t)\phi(x,t), \tag{51}$$

where $\partial_{x_f,x}\tilde{S}_c/\partial_{x_f}^2\tilde{S}_c\approx 1$ was used. The quasiclassical action fulfills the Hamilton-Jacobi equation:

$$-\partial_t\tilde{S}_c=\frac{(\partial_x\tilde{S}_c)^2}{2}-xF(t)+V(x). \tag{52}$$

The saddle-point equations that occur when the x,t integral in Eq. (51) is evaluated are

$$\partial_x\tilde{S}_c=i\kappa-\frac{(Z+\kappa)i}{\kappa x}, \tag{53}$$

$$-\partial_t\tilde{S}_c=-\kappa^2/2+i\frac{F'(t)}{F(t)}, \tag{54}$$

which also define the initial momentum and energy of the ionizing electron. These two equations are inserted into the Hamilton-Jacobi equation yielding a new defining equation for the saddle points,

$$\frac{2i\kappa x_sF'(t_s)}{F(t_s)}+2\kappa x_s^2F(t_s)+\frac{\kappa^2-2\kappa^3x_s+Z^2+2\kappa Z}{\kappa x_s}=0. \tag{55}$$

The latter can be simplified in the limit of $F(t_s)\ll\kappa^3$:

$$x_s\approx\sqrt{\frac{\kappa}{F(t_s)}}. \tag{56}$$

The under-the-barrier trajectory is derived solving Newton equations in the laser and Coulomb fields numerically for different t_s, with the initial coordinate and momentum as a function of the saddle time t_s according to Eqs. (56) and (53). Since we are interested in the peak of the final momentum distribution, the most probable trajectory has to be found, corresponding to a specific t_s. This is accomplished via the additional conditions defining the tunnel exit.

First, for the most probable trajectory, the coordinate should become real at the tunnel exit $\mathrm{Im}\{x(t_e)\}=0$, and second, the electron velocity along the tunneling direction should vanish, $\dot{x}(t_e)=0$. With these boundary conditions, the Coulomb-corrected exit $x(t_e)$ is then deduced from the solutions of the Newton equations and also the asymptotic final momentum $p=\dot{x}(t_f)$ is derived.

An argument can be made for the most probable trajectory as to why the initial electron velocity along the field direction should be vanishing for any γ. First of all, this is the case in SFA with the short-range atomic potential [44]. The Coulomb atomic potential is only a perturbation for the tunneling barrier. In the multiphoton regime additionally this perturbed barrier is oscillating. In this picture, there is no significant physical difference between the Coulomb free case and the case of Coulomb atomic potential. Therefore, one may heuristically apply this assumption also to the case when the Coulomb potential is included.

It is true that different integration contours can be chosen without changing the final electron momentum. For different integration contours, the trajectory of the electron far from the exit is the same, while in close vicinity of the exit, there are still small deviations. Our choice of the contour is based on the physical condition that the electron momentum along the tunneling direction should be vanishing at the tunnel exit. In this way, the most probable trajectory is determined.

The results of HQA are displayed as dots in Figs. 1 and 2. They are in accordance with the classical S_2 CCSFA results. For strong fields, i.e., larger E_s/E_a, HQA gives slightly larger momentum shifts and ionization probabilities. This is due to the fact that in the exact treatment of the Coulomb potential in HQA, the tunneling barrier is smaller than the barrier in the quasiclassical S_2 CCSFA.

Further, we want to note that in the quasiclassical treatments presented here, i.e., in the quasiclassical S_0, S_1, and S_2 SFAs as well as in the HQA, the saddle points in time and in coordinate for the most probable momentum fulfill $\mathrm{Re}\{t_s(p_m)\}=0$ and $\mathrm{Im}\{x_s(p_m)\}=0$ in all considered regimes. This indicates that in a quasiclassical description, tunneling happens instantaneously and there exists neither a static nor a nonadiabatic tunnel-ionization-induced time delay with respect to the laser field maximum.

XI. CONCLUSION

We have investigated the role of high-order corrections in the eikonal CCSFA. There are quasiclassical and quantum second-order corrections to CCSFA. The second-order terms in the quasiclassical S_2 CCSFA decrease the ionization probability and increase the momentum shift. These changes are due to the decreases of the effective tunneling potential barrier of ionization when the Coulomb field of the atomic core is accounted for perturbatively.

There are two types of second-order quantum correction terms which originate either from the S_2 in the eikonal, or the correction term in the prefactor due to high-order terms stemming from S_1. The first term is specific for the 1D problem and absent in the 3D theory. The quantum term in S_2 increases the momentum shift, and the correction term in the prefactor decreases it, yielding to a compensation. However, the compensation is different in the quasistatic and nonadiabatic regimes. While in the quasistatic regime the overall momentum shift is positive, in the nonadiabatic regime the net momentum corrections are negative.

Relating the momentum shift to the ionization delay time at the detector as in the attoclock setup and taking into account that in the 3D case the quantum correction in S_2 is not present, we may conclude that in the 3D case, the variation of the delay time due to the Coulomb field effect will be negative due to the solely determinant correction terms. The fact that time derivatives in the determinant are responsible for the negative

delay time points out that it can be related to the Wigner delay time. Further, one observes that the delay time effect increases in the near-threshold regime, whereas in the deep-tunneling regime it is not significant. This property is characteristic for the tunneling Wigner delay time.

Our approach for CCSFA in the first-order approximation coincides with the ARM theory and demonstrates a simple method to cope with the Coulomb singularity and circumvent the matching procedure of the ARM theory by means of the saddle-point integration of the amplitude not only by time but also by coordinate.

The comparison of our heuristic quasiclassical approach [30] for treating exactly the Coulomb effects for the electron under-the-barrier dynamics during tunneling ionization with the quasiclassical second-order CCSFA shows that the heuristic approach gives slightly larger momentum shifts and ionization probabilities. This stems from a more accurate description of the tunneling barrier in the quasiclassical heuristic method.

ACKNOWLEDGMENTS

E.Y. acknowledges financial support received from the People Programme (Marie Curie Actions) of the European Union's Seventh Framework Programme (FP7/2007-2013) under REA Grant Agreement No. 291734.

[1] C. I. Blaga, F. Catoire, P. Colosimo, G. G. Paulus, H. G. Muller, P. Agostini, and L. F. DiMauro, Nat. Phys. **5**, 1745 (2009).
[2] B. Wolter, M. G. Pullen, M. Baudisch, M. Sclafani, M. Hemmer, A. Senftleben, C. D. Schröter, J. Ullrich, R. Moshammer, and J. Biegert, Phys. Rev. X **5**, 021034 (2015).
[3] P. B. Corkum and F. Krausz, Nat. Phys. **3**, 381 (2007).
[4] F. Krausz and M. Ivanov, Rev. Mod. Phys. **81**, 163 (2009).
[5] L. V. Keldysh, Zh. Eksp. Teor. Fiz. **47**, 1945 (1964) [Sov. Phys. JETP **20**, 1307 (1965)].
[6] F. H. M. Faisal, J. Phys. B **6**, L89 (1973).
[7] H. R. Reiss, Phys. Rev. A **22**, 1786 (1980).
[8] D. M. Wolkow, Z. Phys. **94**, 250 (1935).
[9] W. Becker, F. Grasbon, R. Kopold, D. Milošević, G. G. Paulus, and H. Walther, Adv. Atom. Mol. Opt. Phys. **48**, 35 (2002).
[10] P. Agostini and L. F. D. Mauro, Rep. Prog. Phys. **67**, 813 (2004).
[11] M. Möller, F. Meyer, A. M. Sayler, G. G. Paulus, M. F. Kling, B. E. Schmidt, W. Becker, and D. B. Milošević, Phys. Rev. A **90**, 023412 (2014).
[12] W. Becker and D. B. Milošević, J. Phys. B **48**, 151001 (2015).
[13] Y. Huismans, A. Rouzée, A. Gijsbertsen, J. H. Jungmann, A. S. Smolkowska, P. S. W. M. Logman, F. Lépine, C. Cauchy, S. Zamith, T. Marchenko *et al.*, Science (NY) **331**, 61 (2011).
[14] S. V. Popruzhenko, G. G. Paulus, and D. Bauer, Phys. Rev. A **77**, 053409 (2008).
[15] S. V. Popruzhenko and D. Bauer, J. Mod. Opt. **55**, 2573 (2008).
[16] J. I. Gersten and M. H. Mittleman, Phys. Rev. A **12**, 1840 (1975).
[17] L. Torlina and O. Smirnova, Phys. Rev. A **86**, 043408 (2012).
[18] L. Torlina, M. Ivanov, Z. B. Walters, and O. Smirnova, Phys. Rev. A **86**, 043409 (2012).
[19] J. Kaushal and O. Smirnova, Phys. Rev. A **88**, 013421 (2013).
[20] P. Eckle, A. N. Pfeiffer, C. Cirelli, A. Staudte, R. Dörner, H. G. Muller, M. Büttiker, and U. Keller, Science **322**, 1525 (2008).
[21] A. N. Pfeiffer, C. Cirelli, M. Smolarski, D. Dimitrovski, M. Abu-samha, L. B. Madsen, and U. Keller, Nat. Phys. **8**, 76 (2012).
[22] A. S. Landsman, M. Weger, J. Maurer, R. Boge, A. Ludwig, S. Heuser, C. Cirelli, L. Gallmann, and U. Keller, Optica **1**, 343 (2014).
[23] L. Torlina, F. Morales, J. Kaushal, I. A. Ivanov, A. S. Kheifets, A. Zielinski, A. Scrinzi, H. G. Muller, S. Sukiasyan, M. Ivanov *et al.*, Nat. Phys. **11**, 503 (2015).
[24] E. P. Wigner, Phys. Rev. **98**, 145 (1955).
[25] E. Yakaboylu, M. Klaiber, H. Bauke, K. Z. Hatsagortsyan, and C. H. Keitel, Phys. Rev. A **88**, 063421 (2013).
[26] E. Yakaboylu, M. Klaiber, and K. Z. Hatsagortsyan, Phys. Rev. A **90**, 012116 (2014).
[27] H. K. Avetissian, A. G. Markossian, G. F. Mkrtchian, and S. V. Movsissian, Phys. Rev. A **56**, 4905 (1997).
[28] H. K. Avetissian, K. Z. Hatsagortsian, A. G. Markossian, and S. V. Movsissian, Phys. Rev. A **59**, 549 (1999).
[29] H. K. Avetissian, A. G. Markossian, and G. F. Mkrtchian, Phys. Rev. A **64**, 053404 (2001).
[30] M. Klaiber, K. Z. Hatsagortsyan, and C. H. Keitel, Phys. Rev. Lett. **114**, 083001 (2015).
[31] R. Loudon, Am. J. Phys. **27**, 649 (1959).
[32] R. Loudon, Proc. R. Soc. London A **472**, 20150534 (2016).
[33] G. Abramovici and Y. Avishai, J. Phys. A **42**, 285302 (2009).
[34] M. Klaiber, E. Yakaboylu, and K. Z. Hatsagortsyan, Phys. Rev. A **87**, 023417 (2013).
[35] S. B. Popruzhenko, V. D. Mur, V. S. Popov, and D. Bauer, J. Exp. Theor. Phys. **108**, 947 (2009).
[36] H. Kleinert, *Path Integrals in Quantum Mechanics, Statistics and Polymer Physics* (World Scientific, Singapore, 1990).
[37] A. M. Perelomov and V. S. Popov, Zh. Exp. Theor. Fiz. **52**, 514 (1967) [Sov. Phys. JETP **25**, 336 (1967)].
[38] F. W. J. Olver, *Introduction to Asymptotics and Special Functions* (Academic, New York, 1974).
[39] V. S. Popov, Phys. Usp. **47**, 855 (2004).
[40] This approach named as a simple-man theory was proposed more than 25 years ago in different variations by several authors and proved to have a high predictive power in discussions of strong-field ionization phenomena. See M. Yu. Kuchiev, Pis'ma Zh. Eksp. Teor. Fiz. **45**, 319 (1987) [Sov. Phys. JETP Lett. **45**, 404 (1987)]; H. B. van Linden van den Heuvell and H. G. Muller, in *Multiphoton Processes*, edited by S. J. Smith and P. L. Knight (Cambridge University Press, Cambridge, 1988); K. J. Schafer, B. Yang, L. F. DiMauro, and K. C. Kulander, Phys. Rev. Lett. **70**, 1599 (1993); P. B. Corkum, *ibid.* **71**, 1994 (1993).
[41] S. V. Popruzhenko, V. D. Mur, V. S. Popov, and D. Bauer, Phys. Rev. Lett. **101**, 193003 (2008).
[42] T. Nubbemeyer, K. Gorling, A. Saenz, U. Eichmann, and W. Sandner, Phys. Rev. Lett. **101**, 233001 (2008).
[43] U. Eichmann, T. Nubbemeyer, H. Rottke, and W. Sandner, Nature (London) **461**, 1261 (2009).
[44] M. Li, J.-W. Geng, M. Han, M.-M. Liu, L.-Y. Peng, Q. Gong, and Y. Liu, Phys. Rev. A **93**, 013402 (2016).